

IN SILICO DOCKING AND DYNAMICS OF SELECTED SECONDARY METABOLITES OF *ALBIZIA LEBBECK* AGAINST ANDROGEN RECEPTOR (AR) FOR THE TREATMENT OF PROSTATE CANCER

Ashina Jawahar Nuziba Begum¹, Mageswari Govindaraj¹, Kalpanadevi Murugasamy Maheswari¹, Subhavarshini Raamji¹, Rathish Kumar Sivaraman^{*1}, Helan Soundra Rani Michael³, Vivek Chandramohan², Subashkumar Rathnasamy¹, Shivakumar Bandhumy Lingam¹

Address(es): Rathish Kumar Sivaraman,

¹ Department of Biotechnology, Sri Ramakrishna College of Arts & Science, Coimbatore – 641 006, India.

² SCIOmics, Ooty, India.

³ Department of Biotechnology, Manonmaniam Sundaranar University, Tirunelveli – 627 012, Tamil Nadu, India.

*Corresponding author: rsathishkumar@srcas.ac.in

<https://doi.org/10.55251/jmbfs.10608>

ARTICLE INFO

Received 23. 9. 2023

Revised 18. 10. 2024

Accepted 19. 11. 2024

Published 1. 12. 2024

Regular article



ABSTRACT

Prostate cancer, one of the life-threatening cancers worldwide diagnosed in most elderly men and is influenced by ethnicity, genetic factors, and family history. This article focuses on molecular docking and dynamics simulation for the secondary metabolites (13 compounds) obtained from the methanolic extract of *Albizia lebbek* (L.) Benth against human androgen receptor which plays a crucial role in the progression of cancer and metastasis. Initially, ADMET properties and bioactivity of the ligands were analyzed followed by molecular docking of these ligands and their interactions with the target protein (Androgen Receptor). The compounds 1, 1, 1-Trifluoroheptadecan-2-one and 1-(5-Methylthiophen-2-yl)-N-[(5-methylthiophen-2-yl) methyl] were observed to have the highest binding affinity of -6.8 kcal/mol and -6.5 kcal/mol respectively when compared against the standard, Darolutamide (FDA approved drug) which had a score of -5.1 kcal/mol were taken into consideration. 1, 1, 1-Trifluoroheptadecan-2-on (FLU) and 1-(5-Methylthiophen-2-yl)-N-[(5-methylthiophen-2-yl) methyl] (UND) along with the protein complex were further proceeded with dynamic simulation. The binding energy of FLU and UND system throughout the simulation was studied with an explicit MM-PBSA comparison and was found to be -99.618±14.446 KJ/mol and -117.833±14.838 KJ/mol, influenced by the van der waals energy which was greater in the UND system i.e.-144.227±13.814 KJ/mol than that of the FLU system i.e.-117.054±11.774 KJ/mol. Both the systems were relatively stable with exemplary flexibility and there were no changes in the protein at the structural level during the dynamic simulation. Both FLU and UND systems could become potential therapeutic drugs with further studies.

Keywords: *Albizia lebbek*, Prostate cancer, Androgen receptor, Binding affinity, FLU and UND system

INTRODUCTION

Prostate cancer (PCa) is considered to be one of the most dreadful diseases and has been ranked as the second leading cancer-causing death in males (Murray, 2021). It is often referred to as Adenocarcinoma as the prostate glandular cells are mutated and if not diagnosed at the early stage it localizes and then metastasizes to bones and lymph (Leslie *et al.*, 2023). Elderly men are most prone to be diagnosed with prostate cancer while younger males have rare chances of incidence. Men of African-American origin are most commonly diagnosed with prostate cancer due to the susceptible mutations of a particular gene (chromosome 8q24) (Rawla, 2019). Family history and genetic factors play a crucial role, as proved by the Nordic Twin Study of Cancer (Ng, 2021). Increased consumption of high-calorie food, meat containing saturated fat, food rich in calcium, dairy products, smoking, and consumption of liquor may alter lipid metabolism and cause peroxidation leading to prostate cancer (Chung *et al.*, 2019).

Androgen, a group of steroid hormones is ideally required for the functioning of the prostate gland. Testosterone is the major circulating androgen and 5-alpha dihydrotestosterone (DHT) is the biologically active androgen. Testosterone is metabolized into DHT using the enzyme 5- α reductase (McEwan & Brinkmann, 2021). Testosterone and DHT binds to the intracellular Androgen Receptor (AR), a ligand-dependent nuclear transcription factor with a strong affinity which in turn transactivates the genes for the functioning of male urogenital system receptor secondary signaling cascades (Giona, 2021). Interaction between the AR and DHT is important as one of its three major domains; the DNA binding domain is highly conserved and binds to the selective AR Elements forming a multi-protein transcriptional complex that regulates chromatin remodeling and epigenetic modifications at the AR binding site and promoter region, higher activity of DHT can also leads to prostate cancer. Androgen antagonists resistant to prostate cancer are also associated with AR pathway crosstalk (Davey & Grossmann, 2016). Cells sensitize and mutate the AR which different steroids and ligand-independent nuclear transcriptional factors can activate. The incidence of prostate cancer depends primarily on functional androgen receptors with high transactivation

properties thus AR-mediated signaling occurs in most prostate cancer (Debes & Tindall, 2002). From the Androgen receptor Gene Mutations Database, it can be said that most Prostate cancers were due to somatic mutations and other reasons including mutation in the AR and CpG hotspots.

Albizia lebbek (L.) Benth also called the East Indian Walnut has exhibited varied cytotoxic activities against different cancer types and also increases the level of Caspase-3 and Caspase-8 which aids in apoptosis and also has anti-inflammatory, anti-oxidant, anti-bacterial, and anti-cancer properties (Desai & Joshi, 2019; Malaikolundhan *et al.*, 2020). It is also reported that *A. lebbek* has prominent anti-oxidant activity, possesses neuroprotective properties, and improves motor functions (Saleem *et al.*, 2019). The seeds of *A. lebbek* depicted anti-tumor, anti-fungal, anti-protozoal, and anti-tubercular activities (Lam & Ng, 2011). Moreover, *A. lebbek* was traditionally used in Siddha medicine for its diverse therapeutic importance (Ahmed *et al.*, 2014). Advances in bioinformatics have led to a better understanding of diseases and also aided in prediction of the possible mutations accurately (Beg & Parveen, 2021). The use of NGS (Next-generation Sequencing) has enabled researchers to study the cancer genome and its various associated mutations. A single tissue can be targeted for multiple tests which makes it more beneficial than the conventional Sanger method (Qin, 2019). Molecular docking primarily functions based on the Schrodinger software for lead optimization of hit compounds (Arjun *et al.*, 2020). Molecular docking gives the best conformation for the interacting molecules and the potential drug to compound can be found through simulation against the target protein (Agarwal & Mehrotra, 2016; Fan *et al.*, 2019).

In our present study, we focus on the docking of phytoconstituents of *A. lebbek* to detect the potent metabolites that can inhibit the AR through the binding conformation *in silico* and be compared with standard, FDA-approved drug-Darolutamide. The structures were retrieved from PubChem and were assessed for pharmacokinetic properties in Swiss ADME software and the hit compounds were proceeded with docking and the compounds with best binding scores were taken for simulation.

MATERIALS AND METHODS

Phytochemical structure retrieval

Phytochemicals of *Albizia lebbek* were taken in reference (Anguraj et al., 2024). The compounds obtained from methanolic extraction were taken into consideration for their maximum yield of secondary metabolites and polarity. Out of 21 different phytochemicals, we were able to retrieve 13 phytochemicals from PubChem (<https://pubchem.ncbi.nlm.nih.gov/>). The 2D / 3D structures of *A. lebbek*'s phytochemicals were downloaded in SDF format. Darolutamide, a drug approved by FDA in the year 2019, is an anti-androgen drug and was selected as a standard for which 2D/3D structure was also saved in SDF format (Na'abba et al., 2022).

Analysis of phytochemicals for drug-likeness using Swiss ADME and PASS

The pharmacokinetic properties of the phytochemicals, Lipinski's rule of five (molecular weight, H-bond acceptors, H-bond donors, log P value, and rotatable bonds), Blood Brain Barrier permeability, and bioavailability score were recorded. The compounds following Lipinski's rule of five could possess a drug-likeness nature and were analyzed to screen the hit compounds which are potent drugs using Swiss ADME (<http://www.swissadme.ch/>). The biological activity spectra were used to identify the compound's Pa (Possibility of being active), and Pi (Possibility of being inactive) values, and the previous anti-cancer properties of these compounds were noted using PASS (<http://www.way2drug.com/passonline/>).

Selection of target protein and structure preparation

From the literature search, the crystal structure of the Androgen receptor protein was retrieved from Protein Data Bank (PDB entry: 1E3G) (<https://www.rcsb.org/>) in reference (Abdul-Rida et al., 2021). The protein's original ligand and water molecules were removed using BIOVIA's Discovery Studio Visualizer 2022. The original ligand binding site was considered as a reference binding site for further proceeding (Na'abba et al., 2022).

Molecular docking against the Androgen receptor

Docking aids not only in the prediction of the best conformation of the protein and the ligands but the interactions of the ligands with the active site of the target protein can be analyzed. It is a structure-based drug-designing approach involving the structure preparation of protein and ligands, determining the binding energy of the protein-ligand complex and its analysis (Tripathi & Misra, 2017). 3D structure of the ligands and standard retrieved from PubChem were saved in PDB format (pdbqt) to dock against the human Androgen receptor (1E3G). The grid box was adjusted to cover the active sites of the target protein and the binding ligand (X=12, Y=12, and Z=12) with spacing 1 Å. The binding affinity during the target protein and ligand interactions with a minimum free binding energy was determined using the software Autodock Vina 4.2 (offline open-source software). The confirmation and target protein interactions like hydrophilic interactions, hydrogen bonding, and van der Waals force were analyzed using Discovery Studio Visualizer 2022 (Na'abba et al., 2022).



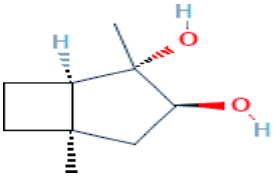
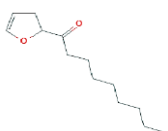
Molecular dynamics (MD) simulation


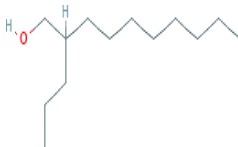

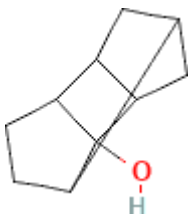
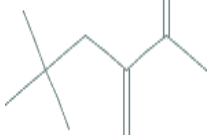
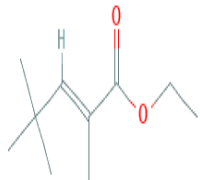
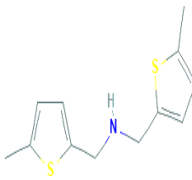
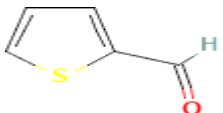

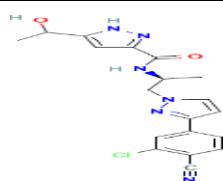
Newton's equations of motion are used in a computational technique known as molecular dynamics (MD) simulation to study the motion of atoms within molecules. In this case, the MD simulation was performed using the widely used and reputable tool Gromacs. In the simulation process, the first step to consider is to reduce the protein-ligand complex. The complex's atomic coordinates are iteratively modified using the steepest descent algorithm to lower the system's potential energy. After minimization, the complex was solvated in a periodic box of water using the SPC water model. The SPC water is a simple model that represents single-point charge water molecules. It is often used as a basis for more complex water models. Furthermore, the complex was maintained at a salt concentration of 0.15 M by incorporating the appropriate sodium and chloride ions concentration. The resulting complex underwent an NPT (constant pressure, constant temperature) equilibration phase before being subjected to a 100 ns (nanoseconds) production run in the NPT ensemble. Using the NPT ensemble, systems with pressure and temperature—often found in biological systems—are simulated. Finally, the simulation's trajectory was examined using the Gromacs software package's tools, which include the protein Root Mean Square Deviation (RMSD), Root Mean Square Fluctuation (RMSF), Radius of Gyration (RG), Solvent Accessible Surface Area (SASA), and H-Bond. Through these experiments, scientists can investigate the structural and dynamic properties of the simulated system, including its general form, flexibility, and interactions with the surrounding solvent. For this experiment, MM-PBSA computations were performed on the target's complex, and the Gromac trajectory of each complex gained 50ns as the final. Gromac was originally used to create topology files and include an explicit solvent to prepare complex structures for calculation. The energy decomposition was carried out on each complex during the final 50 ns of the trajectory after the MM-PBSA computation was configured in the g_ MMPBSA program. To ascertain the binding affinity and the contributions of various energy terms to the total binding energy, the collected energy components were examined.

RESULTS AND DISCUSSION

Phytochemicals are produced because of adaptation to the environment, they widely act as a source for modern pharmaceuticals. Most phytochemicals exist in a biologically active state and few are activated only during stress response (Jain et al., 2019). More than 12% of the drugs are derived from the plant secondary metabolites (Yeshi et al., 2022). The plant secondary metabolites like galantamine, artemisinin, and paclitaxel have been approved to be therapeutic drugs and are used in the treatment of Alzheimer's, malignant cerebral malaria, and ovarian and breast cancer (Twaij & Hasan, 2022). In this study, the 2D/3D structure of *A. lebbek* secondary metabolites and the standard were retrieved from the PubChem database to identify the potent drug-like compound by docking against the target protein (Table 1). The compound's molecular weight ranged from 86.13 /mol to 308.42 g/mol and the molecular weight of the standard (Darolutamide) was 398.8 g/mol.

Table 1 Representation of the ligand's 2D structure with PubChem ID

S.No	Compound Name	PubChem ID	2D Structure	Molecular Formula	Molecular weight (g/mol)
1	Methylnonyl ether	522469		C ₁₀ H ₂₂ O	158.28
2	1,1,1- Trifluoroheptadecan-2-one	4670		C ₁₇ H ₃₁ F ₃ O	308.42
3	(1R,2S,3S,5R)-2,5-Dimethylbicyclo [3.2.0]-heptane-2,3-diol	11040935		C ₉ H ₁₆ O ₂	156.22
4	2-Propyldecan-1-ol	14438907		C ₁₃ H ₂₈ O	200.36

5	Hexacosane	12407		$C_{26}H_{54}$	366.7
6	1-(2,3-Dihydrofuran-2-yl) nonan-1-one	15587435		$C_{13}H_{22}O_2$	210.31
7	Eicosane	8222		$C_{20}H_{42}$	282.5
8	1,3-Methano-5bH-cyclobuta[cd]pentalen-5b-ol, octahydro-	558619		$C_{10}H_{14}O$	150.22
9	2-Methyl-3-(2,2-dimethylpropyl)-butadiene	545358		$C_{10}H_{18}$	138.25
10	Ethyl 2,2,4-trimethylpent-2-enoate	11008363		$C_{10}H_{18}O_2$	170.25
11	1-(5-Methylthiophen-2-yl)-N-[(5-methylthiophen-2-yl) methyl] methanamine	252455		$C_{12}H_{15}NS_2$	237.4
12	Thiophene-2-carboxaldehyde	7364		C_5H_4OS	112.15
13	4-Methoxybut-1-ene	317680		$C_5H_{10}O$	86.13
			Standard		
	Darolutamide	67171867		$C_{19}H_{19}ClN_6O_2$	398.8

ADMET properties and PASS ANALYSIS

Drug discovery and development primarily depend on the ADMET properties. Lipinski's Rule of five is the most preferred rule-based filter for drug discovery during the initial stages (Guan *et al.*, 2019). The activity of a drug in an organism after being administered orally and an understanding of the drug's solubility, permeability, and bioavailability is achieved computationally through ADMET analysis (Flores-Holguin *et al.*, 2021). Androgen receptor being the target, the drug to be compounds must not bypass the Blood Brain Barrier which acts as an obstacle

for drug delivery to the central nervous system as these compounds could be toxic. 1,1,1-Trifluoroheptadecan-2-one, Hexacosane, Eicosane, and 4-Methoxy but-1-ene were not BBB permeant and their main compounds were BBB permeant and were taken into consideration. All the compounds satisfied Lipinski's Rule of five (MW < 500 g/mol, log P < 5, hydrogen bond acceptor < 10, hydrogen bond donor < 5, and rotatable bond < 10) with a good bioavailability score of 0.55. The compounds showed variation insolubility which is given in Table 2.

Table 2 ADMET properties, Lipinski's Rule of Five, and bioavailability score of the selected ligands

S. No	Compound Name	Number of H bond acceptor	Number of H Bond donor	Water solubility	BBB permeant	Rule of Five	Bioavailability score
1	Methylnonylether	1	0	Soluble	Yes	Yes	0.55
2	1,1,1- Trifluoroheptadecan-2-one	4	0	Poorly soluble	No	Yes	0.55
3	(1R,2S,3S,5R)-2,5-Dimethylbicyclo [3.2.0] heptane-2,3-diol	2	2	Very Soluble	Yes	Yes	0.55
4	2-Propyldecan-1-ol	1	1	Moderately soluble	Yes	Yes	0.55
5	Hexacosane	0	0	Poorly Soluble	No	Yes	0.55
6	1-(2,3-Dihydrofuran-2-yl) nonan-1-one	2	0	Moderately Soluble	Yes	Yes	0.55
7	Eicosane	0	0	Poorly Soluble	No	Yes	0.55
8	1,3-Methano-5bH cyclobuta[cd]pental en-5b-ol, octahydro-	1	1	Very Soluble	Yes	Yes	0.55
9	2-Methyl-3-(2,2 dimethylpropyl)-butadiene	0	0	Soluble	Yes	Yes	0.55
10	Ethyl 2,2,4-trimethylpent-2-enoate	2	0	Soluble	Yes	Yes	0.55
11	1-(5- Methylthiophen-2-yl)-N-[(5-methylthiophen-2-yl) methyl] methanamine	1	1	Soluble	Yes	Yes	0.55
12	Thiophene-2-carboxaldehyde	1	0	Very Soluble	Yes	Yes	0.55
13	4-Methoxybut-1-ene	1	0	Very Soluble	No	Yes	0.55

Molecular docking analysis of the ligands against the human androgen receptor. Hydrophobic contacts, hydrogen bonds, and π stacking are the main features of protein-ligand interactions. High-efficiency ligands are primarily composed of hydrophobic interactions (de Freitas & Schapira, 2017; Na'abba et al., 2022). The compounds' binding affinities were examined after the ligands were docked using Autodock Vina 4.2 and attached to the target protein's active sites of the human androgen receptor. The chemicals 1-(5-Methylthiophen-2-yl)-N-[(5-methylthiophen-2-yl) methyl] and 1,1,1-Trifluoroheptadecan-2-one (-6.8 kcal/mol) Table 3 indicates that methanamine (-6.5 kcal/mol) exhibited the highest binding affinity against the active site of protein targets, whereas 4-Methoxybut-1-ene (-3.6 kcal/mol) displayed the lowest binding affinity. The hydrophobic contact with the target site was mostly mediated by the amino acids Met A:742, Phe A:764, Leu A:704, Met A:749, and Met A:745 (1E3G). At the target (1E3G) protein's active region, hexacosane created the greatest number of hydrophobic bonds, while thiophene-2-carboxaldehyde formed the least amount. Six of the total ligands formed H bonds, of which three ligands shared Arg A:752 and Gln A:711, and other amino acids, as listed in Table 4, were also involved in the formation of H bonds at the active site of the target protein, including Asn A:705, Thr A:877, Phe A:764, and Leu A:704.

Table 3 Binding affinity scores of ligands against the target protein (1E3G)

S. No	Compound Name	Pub Chen ID	Binding Score (kcal/mol)
1	Methyl nonyl ether	522469	-4.9
2	1,1,1-Trifluoroheptadecan-2-one	4670	-6.8
3	(1R,2S,3S,5R)-2,5-Dimethylbicyclo [3.2.0] heptane-2,3-diol	11040935	-5.5
4	2-Propyldecan-1-ol	14438907	-5.7
5	Hexacosane	12407	-5.0
6	1-(2,3-Dihydrofuran-2-yl) nonan-1-one	15587435	-6.2
7	Eicosane	8222	-6.0
8	1,3-Methano-5bH-cyclobuta[cd]pentalen-5b-ol, octahydro-	558619	-5.9
9	2-Methyl-3-(2,2-dimethylpropyl)-butadiene	545358	-5.4
10	Ethyl2,2,4-trimethylpent-2-enoate	11008363	-5.4
11	1-(5-Methylthiophen-2-yl)-N- [(5-methylthiophen-2-yl) methyl] methanamine	252455	-6.5
12	Thiophene-2-carboxaldehyde	7364	-4.5
13	4-Methoxybut-1-ene	317680	-3.6
14	Darolutamide (Standard)	67171867	-5.1

Table 4 Hydrophobic interactions and hydrogen bonding of ligands at the active site of the target protein

S. No	PubChem ID	2D structure	Hydrophobic interactions	H bonding
1	522469	 <p>Interactions</p> <ul style="list-style-type: none"> van der Waals Alkyl Pi-Alkyl 	Leu A:704, Phe A:764, MetA:742, MetA:749, Met A:745, Val A:746, Met A:787, Leu A:873, MetA:780	
2	4670	 <p>Interactions</p> <ul style="list-style-type: none"> van der Waals Conventional Hydrogen Bond Carbon Hydrogen Bond Halogen (Fluorine) Alkyl Pi-Alkyl 	Leu A:880, Met A:742, Phe A:876, Leu A:873, MetA: 787, PheA: 764, Ar A: 752, Gln A: 711	
3	11040935	 <p>Interactions</p> <ul style="list-style-type: none"> van der Waals Conventional Hydrogen Bond Alkyl 	LeuA: 873, MetA:742, MetA:745 Leu A:704	
4	14438907	 <p>Interactions</p> <ul style="list-style-type: none"> van der Waals Conventional Hydrogen Bond Carbon Hydrogen Bond Alkyl Pi-Alkyl 	Met A:787, Leu A:873, Val A:746, Leu A:704, MetA:749, LeuA:707, PheA:764	

5

12407



Phe A:764, Met A:745, Leu A:873,
Leu A:704, MetA:895, MetA:742,
Trp A:741, Val A:746, MetA:780,
MetA:749, Leu A:707, Met A:787,
Phe A:876, Leu A:701, LeuA:880

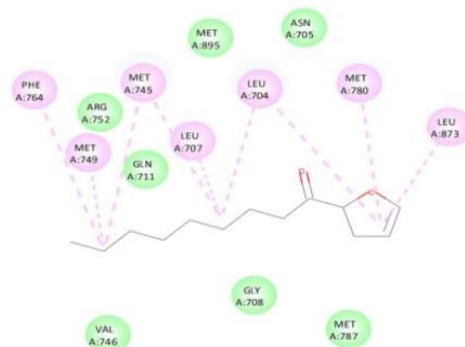
Interactions

van der Waals
Alkyl

Pi-Alkyl

6

15587435



Phe A:764, Met A:749, Met A:745,
Leu A:707, Leu A:704, Met A:780,
LeuA:873

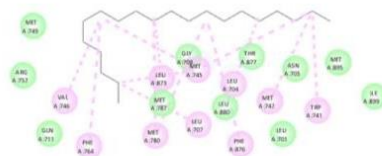
Interactions

van der Waals
Alkyl

Pi-Alkyl

7

8222



Val A:746, Phe A:764, Leu A:873,
Met A:745, Leu A:704, Met A:742,
Trp A:741, Met A:780, LeuA:707,
PheA:876

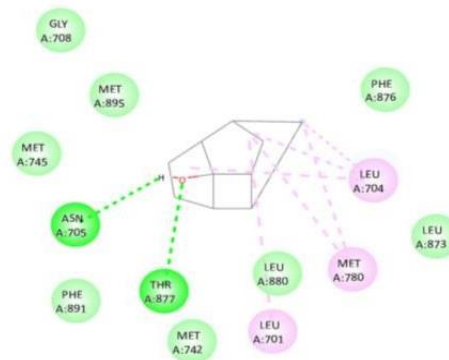
Interactions

van der Waals
Alkyl

Pi-Alkyl

8

558619



LeuA:701, MetA:780, LeuA:704 Asn A:705, ThrA:877

Interactions

van der Waals
Conventional Hydrogen Bond

Alkyl

9	545358	 <p>Leu A:704, Leu A:707, Met A:745, Phe A:764, ValA:746, MetA:749</p>	
10	11008363	 <p>LeuA:704, LeuA:707, PheA:764, Met A:749</p>	
11	252455	 <p>Leu A:880, Leu A:704, Leu A:707, Met A:749, LeuA:701, PheA:764</p>	
12	7364	 <p>MetA:749 Gln A:711, ArgA:752</p>	
13	317680	<p>MetA:745, MetA:787, Phe A:764, Met A:749, ValA: 746</p>	

Rg is used to measure the compactness of the protein's structure. It is the mass-weighted average distance of atoms from the protein's center of mass. The Rg plot displays the changes in the overall shape and folding of a protein throughout a molecular dynamic simulation. The Rg figure in Figure 3 shows how the protein's structure changed at different points during the simulation course. The Rg value pattern of the FLU and UND complexes was consistent throughout the simulation. For the FLU and UND protein complex proteins, the average Rg values from 0 to 100 ns were 2.12 \pm 0.014 nm and 2.11 \pm 0.019 nm, respectively. A helpful metric for assessing the protein complex's structural flexibility is the radius of gyration. The protein complex's Rg values show that the complex's shape folding at various trajectories does not significantly differ from one another. This implies that the protein complex has maintained its structural stability during the simulation.

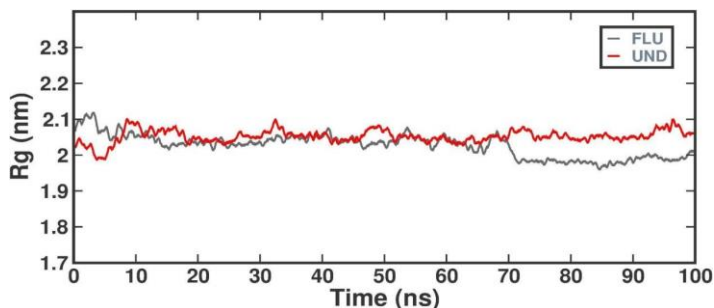


Figure 3 RG of backbone atoms with FLU and UND

The amount of hydrophobic core's compactness was examined in the fluctuation of SASA. Figure 4 illustrates how the SASA of the UND and FLU proteins changes over time. For the FLU and UND protein complex proteins, the average SASA value from 0 to 100 ns was 151.01 \pm 4.45 nm and 150.46 \pm 3.51 nm, respectively. This suggests that the structural level of protein has not changed during the simulation.

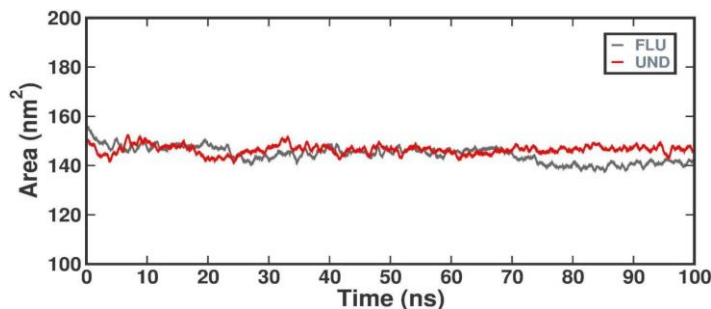


Figure 4 Backbone atoms with FLU and UND in SASA analysis

H Bond

The establishment of H bonds between the protein and ligand was responsible for the stability of the complexes. In this study, simulation analysis was used to validate the H bonds using molecular docking analysis. The results of the H bond analysis for the complexes with FLU and UND are shown in Figure 5.

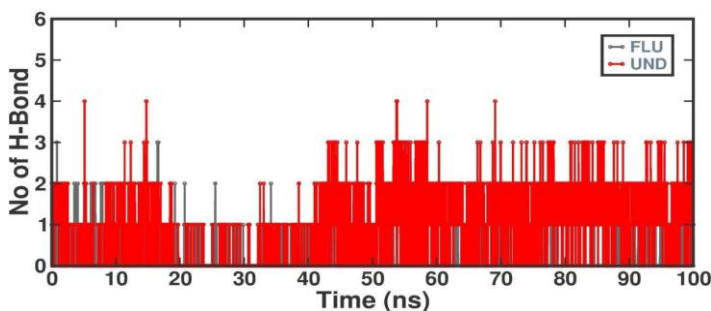


Figure 5 H-Bond of FLU and UND

MM- PBSA

To determine the binding affinities of FLU and UND, the relative binding strengths within the summertime energy protein were examined. As the MM-PBSA method was determined, the binding strengths of FLU and UND to inhibitors were analyzed (Table 5). We calculate contributions to the interaction energy at the residue level throughout a continuous simulation track.

Table 5 Comparison of the binding strength of FLU and UND

System	Vander Waal energy	Electrostatic energy	Polar solvation energy	Binding energy
FLU	-117.054 \pm	-10.320 \pm	41.254 \pm	-99.618 \pm
	11.774kJ/mol	3.518kJ/mol	10.537kJ/mol	14.446 kJ/mol
UND	-144.227 \pm	-29.760 \pm	72.930 \pm	-117.833 \pm
	13.814kJ/mol	12.465kJ/mol	13.520kJ/mol	14.838kJ/mol

The table shows the van der Waals energy, electrostatic energy, polar solvation energy, and binding energy of two systems, FLU and UND. The van der Waals energy of the UND system is significantly higher than the van der Waals energy of the FLU system, with -144.227 kJ/mol versus -117.054 kJ/mol. This is because the UND system has larger molecules, which have more electrons and therefore more van der Waals interactions. The electrostatic energy of the FLU system is significantly lower than the electrostatic energy of the UND system, with -10.320 kJ/mol versus -29.760 kJ/mol. This is because the FLU system has a more negative charge, which means that it experiences more repulsion from the positive charges of the solvent molecules. The polar solvation energy of the UND system is significantly higher than the polar solvation energy of the FLU system, with 72.930 kJ/mol versus 41.254 kJ/mol. This is because the UND system has more polar molecules, which interact more strongly with the polar solvent molecules. The binding energy of the UND system is significantly lower than the binding energy of the FLU system, with -117.833 kJ/mol versus -99.618 kJ/mol. This is because the UND system has a larger van der Waals radius, which means that it is less tightly bound to the solvent molecules. Overall, the table shows that the UND system has weaker interactions with the solvent molecules than the FLU system. This is likely due to the larger size and more negative charge of the UND molecules.

CONCLUSION

In our present study, we focused on the molecular docking and dynamics of *Albizia lebbek*'s secondary metabolites. The ADMET properties of the phytochemicals were analyzed majorly focusing on the Lipinski's Rule of five which is considered to be the most basic qualification or any potential drug to be compounds and gives a good bioavailability score. All the compounds followed the Rule of five and had a bioavailability score of 0.55. The previous anti-cancer activity of the compounds

was checked in consideration with the Pa and Pi score and preceded with molecular docking. From the results, the compounds with highest binding affinity; 1,1,1-Trifluoroheptadecan-2-one (FLU) (-6.8 kcal/mol) and 1-(5-Methylthiophen-2-yl)-N-[(5-methylthiophen-2-yl) methyl] methanamine (UND) (-6.5 kcal/mol) was performed with MD simulation. From the RMSD result, the FLU and UND systems were found to be stable throughout the simulation. The RMSF, Rg, SASA and H bonding results suggest that there were no structural changes in the protein with both the systems being structurally stable. The UND system had less binding energy with the solvent molecules when compared to the FLU system owing to the greater van der waals force which was comparatively larger in the UND system. Considering all these, the compounds 1, 1, 1-Trifluoroheptadecan-2-one and 1-(5-Methylthiophen-2-yl) -N- [(5-methylthiophen-2-yl) methyl] can be taken for further *in vitro* studies.

Conflict of interest: The authors declare that there are no conflicts of interest.

REFERENCES

- Murray, T. B. (2021). The pathogenesis of prostate cancer. *Exon Publications*, 29-41. <http://dx.doi.org/10.36255/exonpublications.prostatecancer.pathogenesis.2021>
- Leslie, S. W., Sajjad, H., & Villanueva, C. A. (2023). Cryptorchidism, Continuing Education Activity. Treasure Island (FL): StatPearls Publishing. <https://www.statpearls.com/>
- Rawla, P. (2019). Epidemiology of prostate cancer. *World journal of oncology*, 10(2), 63. <https://doi.org/10.14740/wjon1191>
- Ng, K. L. (2021). The Etiology of prostate cancer. *Exon Publications*, 17-27. <https://doi.org/10.36255/exonpublications.prostatecancer.etiology.2021>

- Chung, B. H., Horie, S. & Chiong, E. (2019). The incidence, mortality, and risk factors of prostate cancer in Asian men. *Prostate international*, 7(1), 1-8. <https://doi.org/10.1016/j.prmil.2018.11.001>
- McEwan, I. J. & Brinkmann, A. O. (2021). Androgen Physiology: Receptor and Metabolic Disorders. [Updated 2021 Jul 2]. In: Feingold KR, Anawalt B, Blackman MR, et al., editors. Endotext. South Dartmouth (MA): MDText.com, Inc.; 2000. <https://www.ncbi.nlm.nih.gov/books/NBK279028/>
- Giona, S. (2021). The Epidemiology of Prostate Cancer. In: Bott SRJ, Ng KL, editors. Prostate Cancer [Internet]. Brisbane (AU): Exon Publications; 2021 May 27. Chapter 1. <https://doi.org/10.36255/exonpublications.prostatecancer.epidemiology.2021>
- Davey, R. A. & Grossmann, M. (2016). Androgen Receptor Structure, Function and Biology: from Bench to Bedside. *The clinical biochemist reviews*, 37(1), 3. <https://pubmed.ncbi.nlm.nih.gov/27057074/>
- Debes, J. D. & Tindall, D. J. (2002). The role of androgens and the androgen receptor in prostate cancer. *Cancer letters*, 187(1-2), 1-7. [https://doi.org/10.1016/s0304-3835\(02\)00413-5](https://doi.org/10.1016/s0304-3835(02)00413-5)
- Desai, T. H. & Joshi, S. V. (2019). Anticancer activity of saponin isolated from *Albizia lebbbeck* using various *in vitro* models. *Journal of ethnopharmacology*, 231, 494-502. <https://doi.org/10.1016/j.jep.2018.11.004>
- Malaikolundhan, H., Mookkan, G., Krishnamoorthi, G., Matheswaran, N., Alsawalha, M., Veeraraghavan, V.P., Krishna Mohan, S. & Di, A. (2020). Anticarcinogenic effect of gold nanoparticles synthesized from *Albizia lebbbeck* on HCT-116 colon cancer cell lines. *Artificial cells, Nanomedicine, and Biotechnology*, 48(1), 1206-1213. <https://doi.org/10.1080/21691401.2020.1814313>
- Saleem, U., Raza, Z., Anwar, F., Chaudary, Z. & Ahmad, B. (2019). Systems pharmacology based approach to investigate the *in vivo* therapeutic efficacy of *Albizia lebbbeck* (L.) in experimental model of Parkinson's disease. *BMC complementary and alternative medicine*, 19 (1), 1-16. <https://doi.org/10.1186/s12906-019-2772-5>
- Lam, S. K. & Ng, T. B. (2011). First report of an anti-tumor, anti-fungal, anti-yeast and anti-bacterial hemolysin from *Albizia lebbbeck* seeds. *Phytomedicine*, 18(7), 601-608. <https://doi.org/10.1016/j.phymed.2010.08.009>
- Ahmed, D., Kumar, V., Sharma, M. & Verma, A. (2014). Target guided isolation, *in vitro* antidiabetic, antioxidant activity and molecular docking studies of some flavonoids from *Albizia Lebbbeck* Benth. bark. *BMC complementary and alternative medicine*, 14, 1-13. <https://doi.org/10.1186/1472-6882-14-155>
- Beg, A. & Parveen, R. (2021). Role of bioinformatics in cancer research and drug development. In *Translational bioinformatics in healthcare and medicine* 141-148. Academic Press. <http://dx.doi.org/10.1016/B978-0-323-89824-9.00011-2>
- Qin, D. (2019). Next-generation sequencing and its clinical application. *Cancer biology & medicine*, 16(1), 4. <https://doi.org/10.20892%2Fj.issn.2095-3941.2018.0055>
- Arjun, H. A., Rajan, R. K., Elancheran, R., Ramanathan, M., Bhattacharjee, A. & Kabilan, S. (2020). Crystal structure, Hirshfeld surface analysis, DFT and molecular docking studies on benzohydrazide derivatives as potential inhibitors of prostate cancer. *Chemical Data Collections*, 26, 100350. <http://dx.doi.org/10.1016/j.cdc.2020.100350>
- Agarwal, S. & Mehrotra, R. J. J. C. (2016). An Overview of Molecular Docking. *JSM chem*, 4(2), 1024-1028.
- Fan, J., Fu, A. Zhang, L. (2019). Progress in molecular docking. *Quantitative Biology*, 7, 83-89. <https://doi.org/10.1007/s40484-019-0172-y>
- Anguraj, A., Michael, M.H.S., Sugumaran, S., Madhusudhanan, G. R. & Sivaraman, R.K. (2024). A comparative study on biosynthesized silver nanoparticles from *H. undatus* fruit peel and their therapeutic applications. *Discover Nano*, 19(49). <https://doi.org/10.1186/s11671-024-03995-w>
- Na'abba, Z. U., Datti, I. G., Kumar, P. T., Sabo, H. M. & Auwal, M. A., 2022. Molecular Docking Analysis of *Azadirachta Indica* Phytocompounds against Androgen Receptor Protein for the Treatment of Prostate Cancer. *Journal of Biotechnology*, 1(1), 9-36. <http://dx.doi.org/10.36108/jbt/2202.10.0120>
- Abdul-Rida, N. A., Farhan, A. M., Al-Masoudi, N. A., Saeed, B. A., Miller, D. & Lin, M. F. (2021). A novel pregnene analogs: synthesis, cytotoxicity on prostate cancer of PC-3 and LNCaP-AI cells and *in silico* molecular docking study. *Molecular diversity*, 25, 661-671. <https://doi.org/10.1007/s11030-020-10038-w>
- Tripathi, A. & Misra, K. (2017). Molecular docking: A structure-based drug designing approach. *JSM Chem*, 5(2), 1042-1047.
- Jain, C., Khatana, S. & Vijayvergia, R. (2019). Bioactivity of secondary metabolites of various plants: a review. *Int. J. Pharm. Sci. Res*, 10(2), 494-504. [http://dx.doi.org/10.13040/IJPSR.0975-8232.10\(2\).494-04](http://dx.doi.org/10.13040/IJPSR.0975-8232.10(2).494-04)
- Yeshe, K., Crayn, D., Ritmejeriyé, E. & Wangchuk, P. (2022). Plant secondary metabolites produced in response to abiotic stresses has potential application in pharmaceutical product development. *Molecules*, 27(1), 313. <https://doi.org/10.3390/molecules27010313>
- Twaij, B. M. & Hasan, M. N. (2022). Bioactive secondary metabolites from plant sources: Types, synthesis, and their therapeutic uses. *International Journal of Plant Biology*, 13(1), 4-14. <https://doi.org/10.3390/ijpb13010003>
- Guan, L., Yang, H., Cai, Y., Sun, L., Di, P., Li, W., Liu, G. & Tang, Y. (2019). ADMET-score-a comprehensive scoring function for evaluation of chemical drug-likeness. *Medchem comm*, 10(1), 148-157. <https://doi.org/10.1039%2Fc8md00472b>
- Flores-Holguín, N., Frau, J. & Glossman-Mitnik, D. (2021). Computational Pharmacokinetics Report, ADMET Study and Conceptual DFT-Based Estimation of the Chemical Reactivity Properties of Marine Cyclopeptides. *Chemistry Open*, 10(11), 1142-1149. <https://doi.org/10.1002%2Fopen.202100178>
- de Freitas, R. F. & Schapira, M. (2017). A systematic analysis of atomic protein-ligand interactions in the PDB. *Medchem comm*, 8(10), 1970-1981. <https://doi.org/10.1039/C7MD00381A>
- Hollingsworth, S. A. & Dror, R. O. (2018). Molecular dynamics simulation for all. *Neuron*, 99(6), 1129-1143. <https://doi.org/10.1016/j.neuron.2018.08.011>
- Liu, X., Shi, D., Zhou, S., Liu, H., Liu, H. & Yao, X. (2018). Molecular dynamics simulations and novel drug discovery. *Expert opinion on drug discovery*, 13(1), 23-37. <https://doi.org/10.1080/17460441.2018.1403419>